Supporting Information for

Atmospheric photosensitization: a new pathway for sulfate formation

Xinke Wang[†], Rachel Gemayel[†], Nathalie Hayeck[†], Sebastien Perrier[†], Nicolas Charbonnel[†], Caihong Xu[‡], Hui Chen[‡], Chao Zhu[‡], Liwu Zhang[‡], Lin Wang[‡], Sergey A. Nizkorodov[§], Xinming Wang[‖], Zhe Wang[⊥], Tao Wang[⊥], Abdelwahid Mellouki[#], Matthieu Riva[†], Jianmin Chen[‡,¶,*], Christian George[†,*]

[†]Univ Lyon, Université Claude Bernard Lyon 1, CNRS, IRCELYON, F-69626, Villeurbanne, France.

[‡]Shanghai Key Laboratory of Atmospheric Particle Pollution and Prevention (LAP[3]), Department of Environmental Science & Engineering, Institute of Atmospheric Sciences, Fudan University, Shanghai 200438, China.

[§]Department of Chemistry, University of California, Irvine, Irvine, California, 92697, USA.

[‖]State Key Laboratory of Organic Geochemistry and Guangdong province Key Laboratory of Environmental Protection and Resources Utilization, Guangzhou Institute of Geochemistry, Chinese Academy of Sciences, Guangzhou 510640, China

[⊥]Department of Civil and Environmental Engineering, The Hong Kong Polytechnic University, Hong Kong 999077, China.

[#]Institut de Combustion, Aérothermique, Réactivité et Environnement (ICARE), CNRS/OSUC, 45071 Orléans Cedex 2, France

[¶]Institute of Eco-Chongming, 3663 Zhongshan Road, Shanghai 200062, China

[*]To whom correspondence should be addressed. Email: christian.george@ircelyon.univ-lyon1.fr, Email : jmchen@fudan.edu.cn

This PDF file includes:

Pages S1 to S18

Supplementary Information text

Figs. S1 to S4

Tables S1 to S3

Other Supplementary Material for this manuscript includes the following:

Database S1

Supplementary Information text

Filter samples chemical analysis. For the UPLC separation, more details can be found in the previous study.[1] In brief, ambient aerosol extracts were separated using a Waters Acquity HSS T3 column (1.8 μm, 2.1 × 100 mm) with acidified water (eluent A; 0.1%, v/v, formic acid) and acidified acetonitrile (eluent B; 0.1%, v/v, formic acid). PFBHA derivatization was used to identify organic compounds with carbonyl functional groups.[1] Two hundred μL of the extracts were mixed with 800 μL of PFBHA solutions (1 mg/mL), then was left in darkness at room temperature for 24 h. However, the gradient elution procedure for PFBHA derivatives was different: eluent B increased from 30% to 100% in 15 min, then was kept 100% for 2.5 min, and lastly returned to 30% and stabilized for 2.5 min. UV-Vis absorption was measured using the DAD over the wavelength range of 190-798 nm. For the HRMS analysis, HESI voltages of -3 and 3 kV were applied for negative and positive ionization mode (ESI- and ESI+) measurements, respectively. Additionally, the sheath gas flow rate was set to 60 arbitrary units (au) and the auxiliary gas flow rate to 20 au. A capillary temperature of 300 °C and a heater temperature of 400 °C were used. All measurements were performed using the highest mass resolution (R = 140,000 at *m/z* 200) and the scanning range was set to *m/z* 50-750. However, carbonyl-containing compounds with high molecular weight (> 554 Da) could not be differentiated using PFBHA derivatization due to the mass limitation of scanning range.

For the data analysis, Xcalibur 2.2 (Thermo, USA) and MZmine 2.33 were used. Formula assignments of the identified signals were achieved using mass tolerances of 2 ppm error in the ESI- and 3 ppm error in the ESI+. Moreover, more restrictions for formula assignments and LC-MS data processing are given in Tables S2-S3. Chromophores have also been distinguished by

examining time periods of the UPLC-HRMS data corresponding to the DAD absorption peaks (Fig. S2).

The setup and principle of the pulsed laser system. The centerpiece of the experimental set-up is a Liquid Core Waveguide (LCW) made of Teflon AF 2400 (BioGeneral, San Diego, CA). Such a type of material has been shown to exhibit excellent optical properties such as high optical clarity (at $\lambda > 200$ nm more than 80% of light is transmitted through a 220 μm thick film of the polymer described above) and very low refractive index (i.e., n=1.29 for Teflon AF 2400 grades). As a result, once filled with water, the tubing will have the properties of a fiber optic waveguide. The Teflon AF 2400 guide has an inner and outer diameter of 0.6 mm and 0.8 mm, respectively, a length of 100 cm with an inner volume of 0.28 mL. This very small liquid volume represents the major advantage of the waveguides compared to standard cells.

The highly flexible Teflon AF 2400 tubing was loosely coiled (less than 3 cm diameter) and placed in the diverging laser beam path. Triplet states were generated within the LCW following the laser flash of the precursors discussed above. As the waveguide was used as a coil, no concentration gradient could build up along the waveguide length. However, non-uniform transient concentration can be produced if the laser fluence on the coil is not uniform. To optimize uniformity of the illumination of the front and back sides of the waveguide, we placed it inside a small box (1×3×3 cm^3 height×width×depth) with inner walls coated by aluminum foil. This ensured a better irradiation of the waveguide, however, in this configuration the fluence could not be easily measured. Consequently, we made sure that all kinetics studied were unimolecular.

A peristaltic pump was used to transport the solutions at a flow of 1.6 mL min^{-1}, and all connections were made of PTFE materials. The solution content of the Teflon photolysis cell was probed by spectrophotometry. The output of a 150 W high-pressure Xenon arc lamp was focused

on the entry of an unpolished 500-μm diameter fused silica optical fiber. The fiber delivered the broadband radiation from the Xe-lamp to the entrance of the liquid core waveguide. The Teflon AF tubing conducted the radiation up to its end where another fused silica optical fiber (located in the liquid) collected some of this transmitted radiation and projected it on a slit of ¼ m monochromator (Spectral Products DK240) equipped with a 2400 grooves/mm grating, and a photomultiplier tube detector (Hamamatsu H7732-01). The photo-multiplier signal was passed through a high-speed current amplifier/discriminator (Femto) and the AC component recorded on a 300 MHz oscilloscope (Tektronix TDS3032c). The digitized signals were eventually transferred to a microcomputer for further analysis. Measurements were repeated every 10-15 nm between 350 and 650 nm to construct the absorption spectrums.

Sulfate production rate calculations. Sulfate production rates were calculated for different aqueous-phase reaction pathways with O_3, H_2O_2, TMIs and NO_2, according to the detailed description made by Cheng et al.,[2] and briefly reproduced below.

For the "Beijing haze" scenario, the following input parameters were used: $[PM_{2.5}]$ = 300 μg m^{-3}, $[SO_2\ (g)]$ = 40 ppb, $[NO_2\ (g)]$ = 66 ppb, $[H_2O_2\ (g)]$ = 0.25 ppb,[3] $[O_3\ (g)]$ = 1 ppb, aerosol water content (AWC) = 300 μg m^{-3}, aerosol droplet radius R_p = 0.15 μm, and T = 271 K. The total soluble Fe and Mn were used as 18 and 42 ng m^{-3}, but their exact concentrations are pH-dependent and obtained from the following equations:

$$[Fe(III)] = \frac{K_{sp,Fe(OH)3}}{[OH^-]^3} \text{ and } [Mn(II)]_{sat} = \frac{K_{sp,Mn(OH)2}}{[OH^-]^2} \qquad \text{(Eq. S1)}$$

where $K_{sp,\ Fe\ (OH)3}$ and $K_{sp,\ Mn\ (OH)2}$, the precipitation constants of $Fe(OH)_3$ and $Mn(OH)_2$, are 6×10^{-38} and 1.6×10^{-13}, respectively.[4] The physical Henry's constants (H, M atm^{-1}) of SO_2, O_3, H_2O_2, and NO_2 are 1.23, 1.1×10^{-2}, 1.0×10^{5}, and 1.0×10^{-2}, respectively, so their concentrations in the liquid

phase could be calculated based on the Henry's law. In addition, the temperature dependent Henry's constants can be calculated as:

$$H(\mathrm{T}) = H(T_0)\exp\left[-\frac{\Delta H_{298K}}{R}\left(\frac{1}{T}-\frac{I}{T_0}\right)\right] \quad \text{(Eq. S2)}$$

where the $-\Delta H_{298K}/R$ normalized enthalpy of dissolution values for SO_2, O_3, H_2O_2, and NO_2 are 3.1×10^3, 2.5×10^3, 7.3×10^3, and 2.5×10^3 (K), respectively. The dissociation equilibrium constants (K) for the Eq. 2 in the main text (K_{s1}) and the Eq. 3 (K_{s2}) are 1.3×10^{-2} M and 6.6×10^{-8} M at 298K.

The following rate laws for the sulfate production rate (R_{aq}) calculations were used, again according to Cheng et al.[2]

- by ozone:

$$\frac{d[SO_4^{2-}]}{dt} = (k_1[SO_2\cdot H_2O] + k_2[HSO_3^-] + k_3[SO_3^{2-}])[O_3(aq)] \quad \text{(Eq. S3)}$$

where $k_1 = 2.4\times10^4$ $M^{-1}s^{-1}$, $k_2 = 3.7\times10^5$ $M^{-1}s^{-1}$, $k_3 = 1.5\times10^9$ $M^{-1}s^{-1}$.

- by H_2O_2:

$$\frac{d[SO_4^{2-}]}{dt} = \frac{k_4[H^+][HSO_3^-][H_2O_2]}{1+K[H^+]} \quad \text{(Eq. S4)}$$

where $k_4 = 7.45\times10^7$ $M^{-2}s^{-1}$, $K = 13$ M^{-1}.

- by the transition metal ions:

$$\mathrm{pH} \le 4.2,\ \frac{d[SO_4^{2-}]}{dt} = k_5[H^+]^{-0.74}[Mn(II)][Fe(III)][S(IV)] \quad \text{(Eq. S5)}$$

$$\mathrm{pH} > 4.2,\ \frac{d[SO_4^{2-}]}{dt} = k_6[H^+]^{0.67}[Mn(II)][Fe(III)][S(IV)] \quad \text{(Eq. S6)}$$

where $k_5 = 3.72\times10^7$, $k_6 = 2.51\times10^{13}$.[5]

- by NO_2:

$$\frac{d[SO_4^{2-}]}{dt} = k_7[NO_2(aq)][S(IV)] \quad \text{(Eq. S7)}$$

where k_7 could be two different values based on two studies (Cheng et al.[2] and references therein), $k_{7,\ low}$ = (0.14~2) $\times 10^6$ $M^{-1}s^{-1}$ or $k_{7,\ high}$ = 2.51×10^{13} $M^{-1}s^{-1}$. In this calculation, the average rate calculated by $k_{7,\ low}$ and $k_{7,\ high}$ were used following Cheng et al.[2]

- Finally, for the T* oxidation pathway, we used:

$$\frac{d[SO_4^{2-}]}{dt} = k_q[T^*]([SO_2 \cdot H_2O] + [HSO_3^-]) \quad \text{(Eq. S8)}$$

where k_q = 1.3×10^8 $M^{-1}s^{-1}$ calculated based on Fig. 3.

It should be noted that the kinetics for TMIs and T^* oxidation pathways were used at 298 K due to the lack of the information on E/R, which would be overestimated for the sulfate production rates during the Beijing winter haze scenario (271 K). For the influences of ionic strength on aqueous sulfate-producing reactions, the rate constants were taken as for diluted solutions.[2]

Figures and Tables

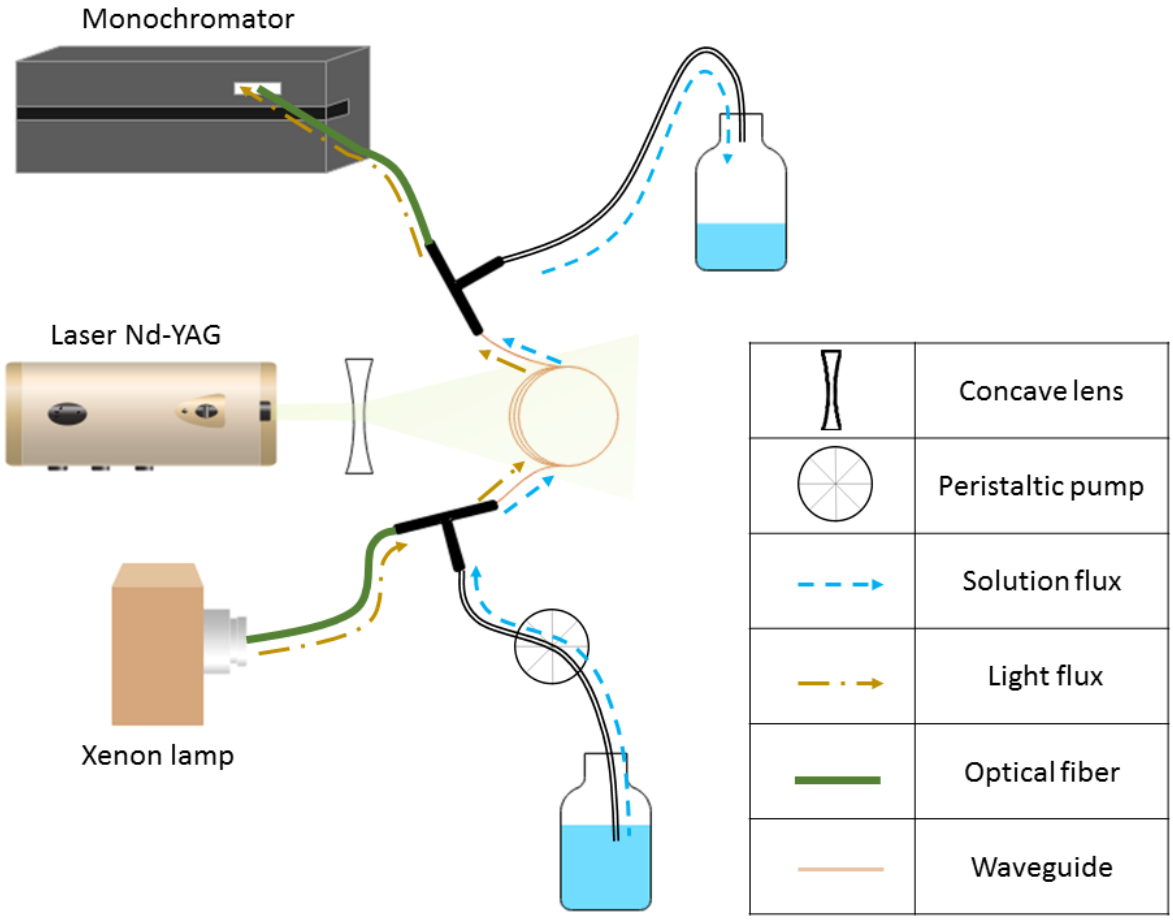

Fig. S1. Schematic of the pulsed laser excitation system.

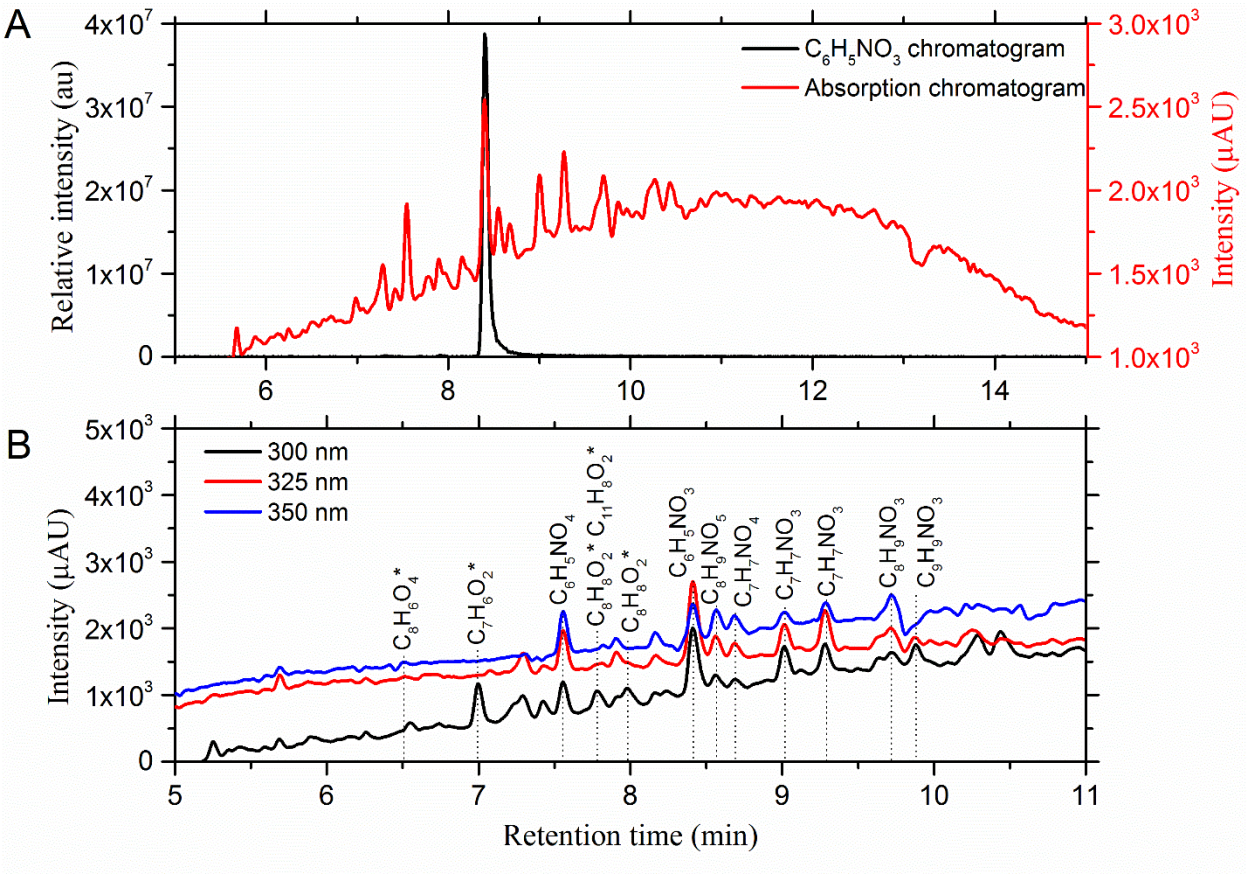

Fig. S2. UPLC-DAD absorption and ion chromatograms. (**A**) An example demonstrating the method used for identification of a potential chromophore ($C_6H_5NO_3$) responsible for light absorption (290-350 nm). (**B**) The selected blank-subtracted absorption chromatograms at 300, 325, and 350 nm. The peaks were labeled by the formulas of the probable chromophores. * A molecule contains at least one carbonyl functional group.

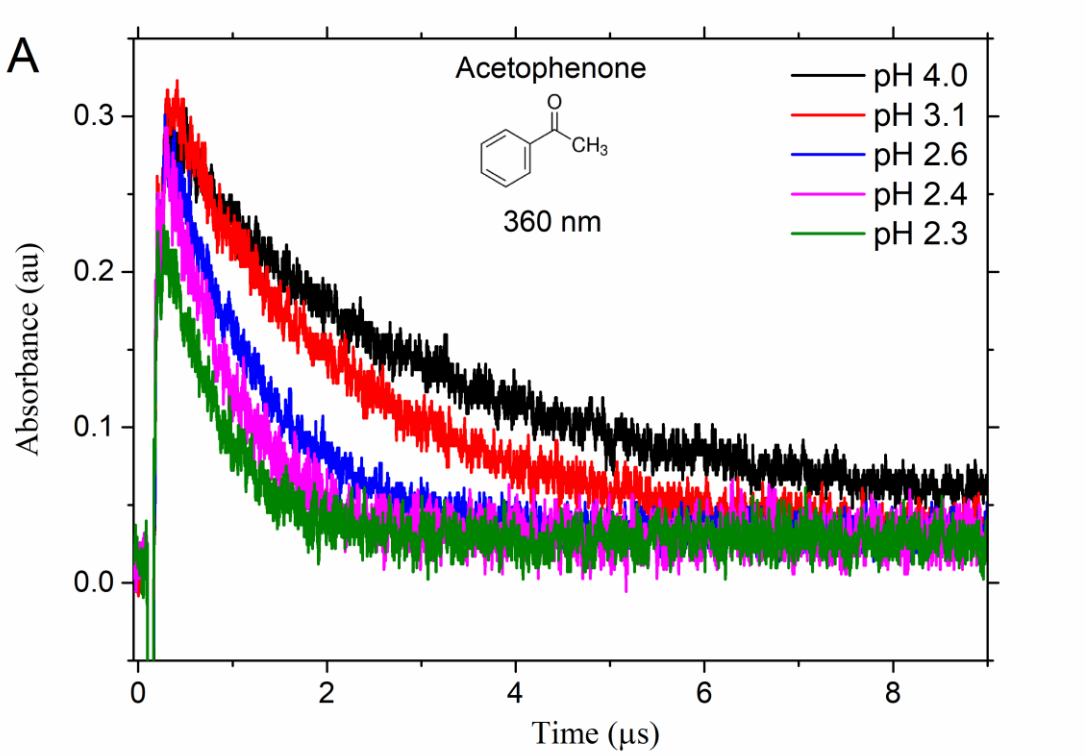
A
Acetophenone
360 nm
pH 4.0
pH 3.1
pH 2.6
pH 2.4
pH 2.3
Absorbance (au)
Time (μs)

140

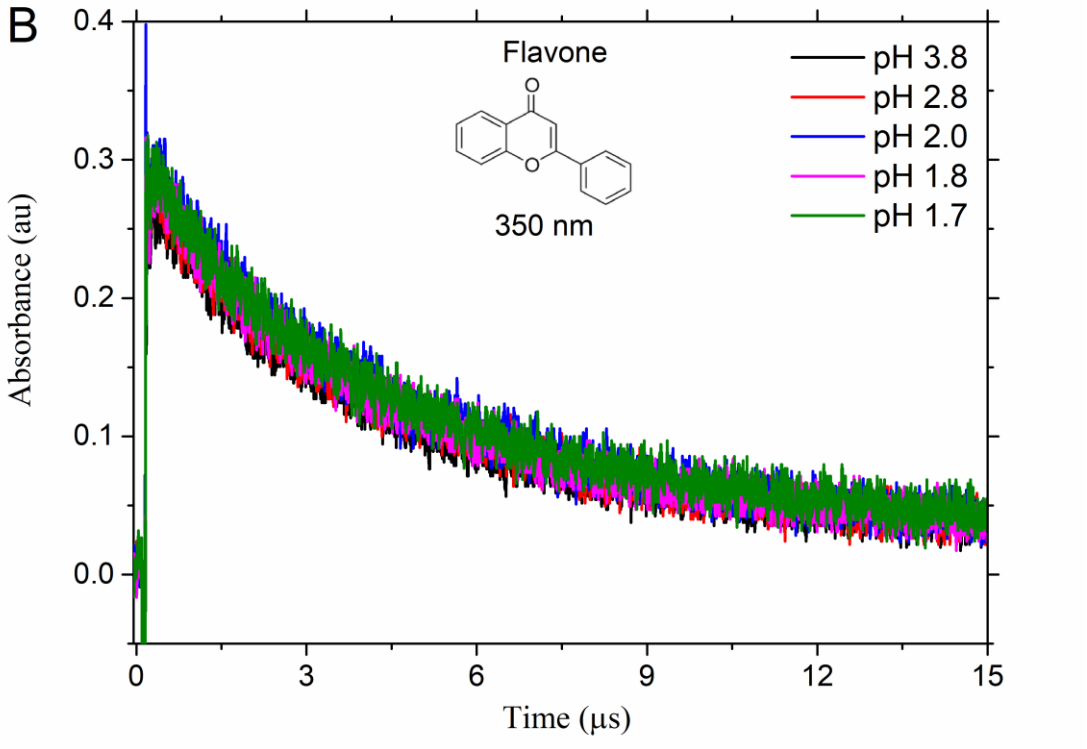
B
Flavone
350 nm
pH 3.8
pH 2.8
pH 2.0
pH 1.8
pH 1.7
Absorbance (au)
Time (μs)

141

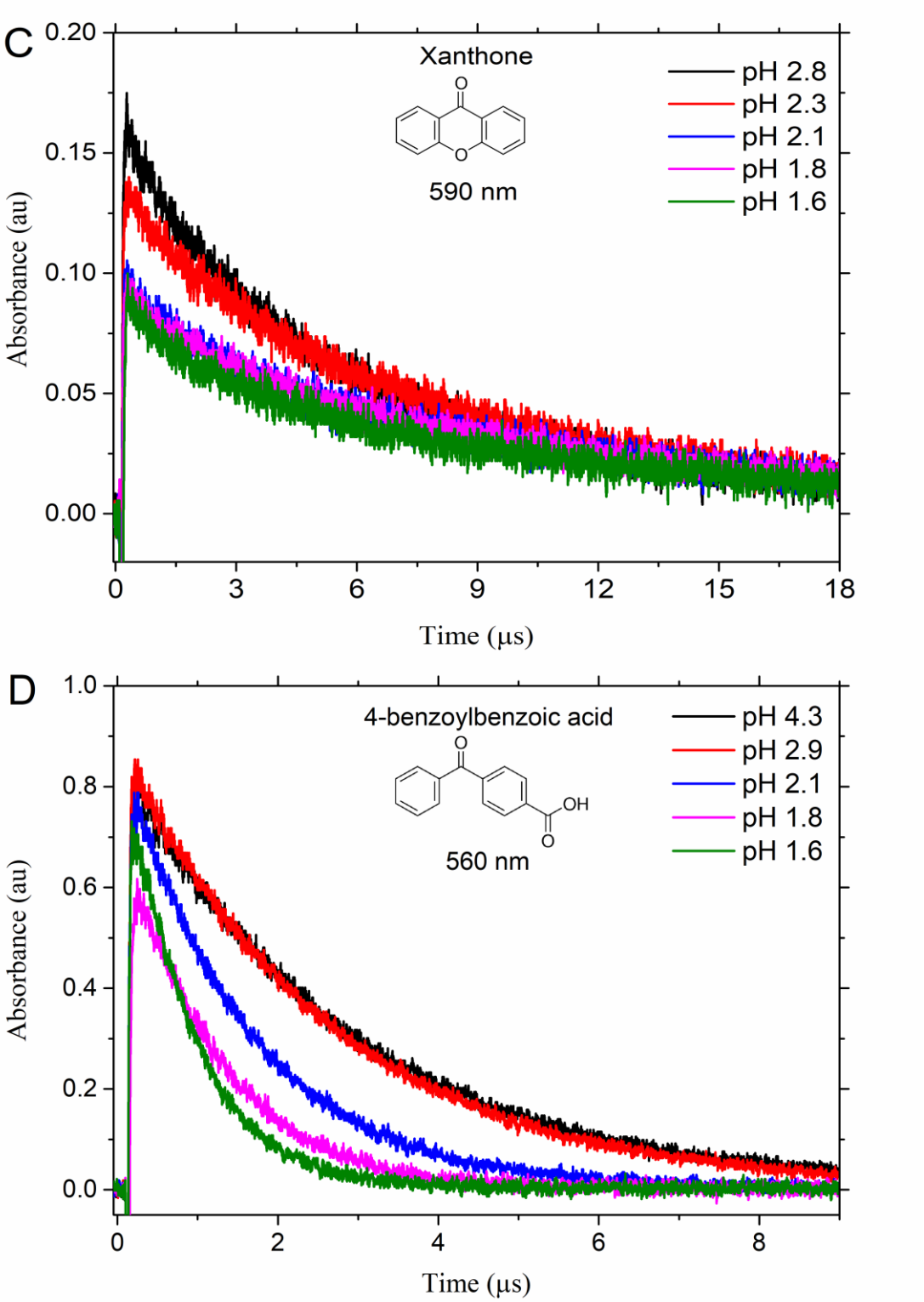

Fig. S3. Transient absorption decays of (A) acetophenone, (B) flavone, (C) xanthone, and (D) 4-BBA triplet state in deoxygenated aqueous solutions without S(IV) but at different pH, respectively.

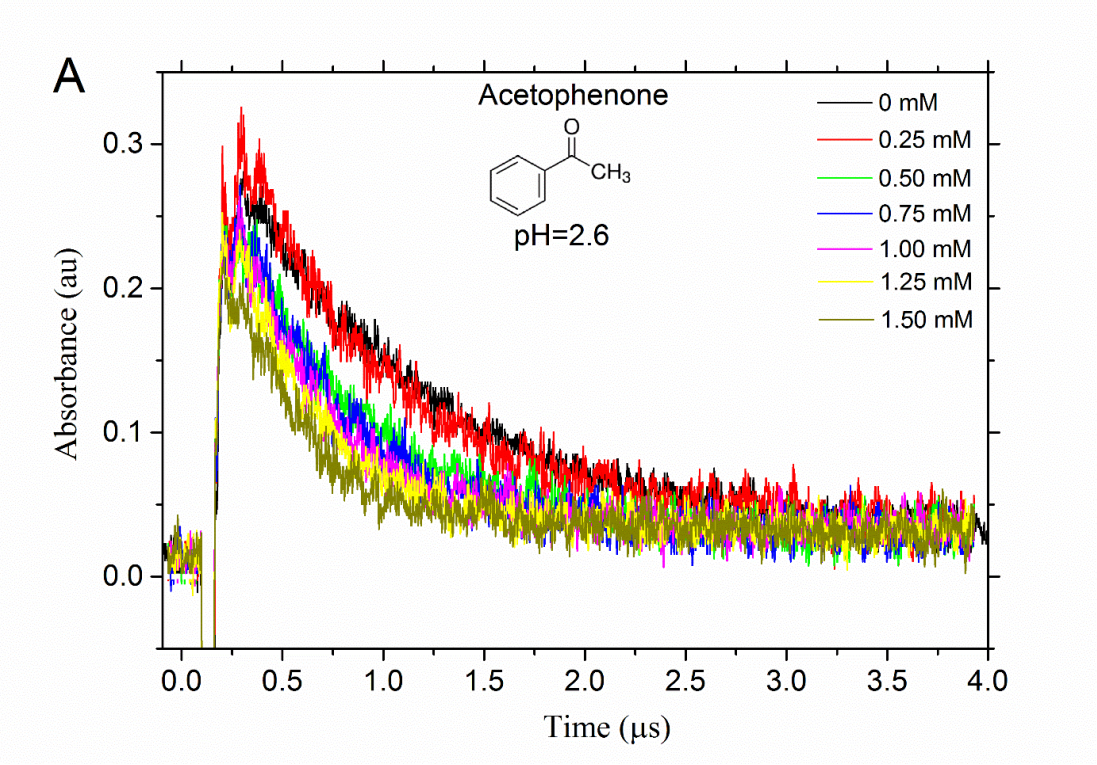
A
Acetophenone
O
CH3
pH=2.6
0 mM
0.25 mM
0.50 mM
0.75 mM
1.00 mM
1.25 mM
1.50 mM
Absorbance (au)
0.0
0.1
0.2
0.3
0.0
0.5
1.0
1.5
2.0
2.5
3.0
3.5
4.0
Time (μs)

149

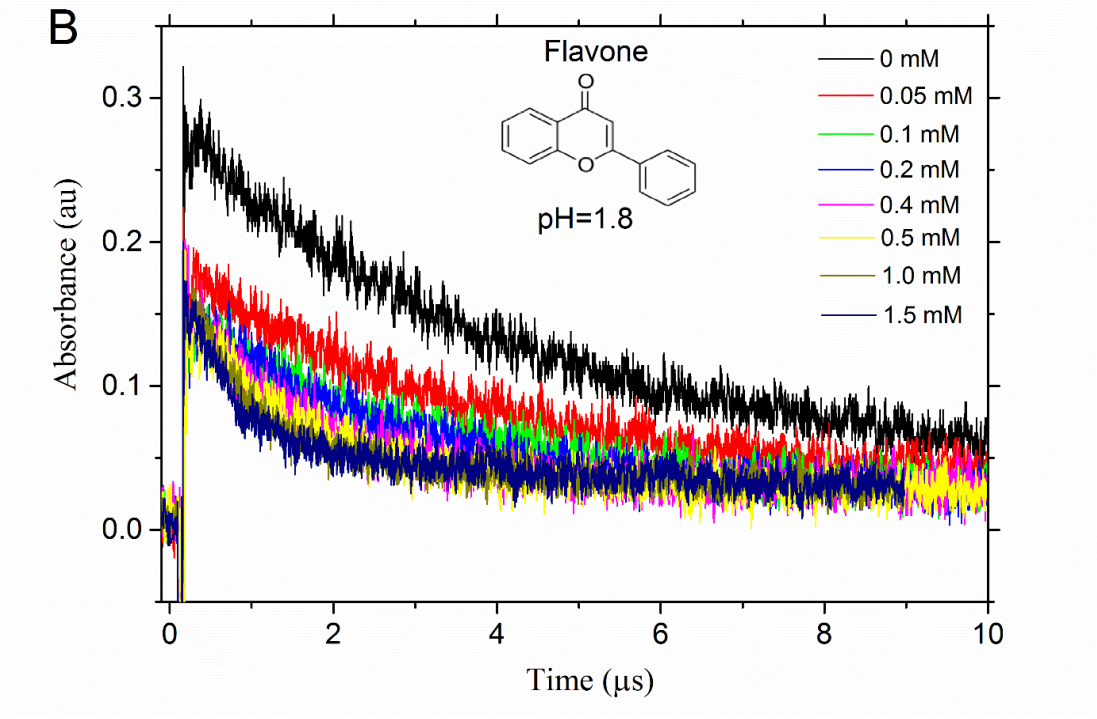
B
Flavone
O
O
pH=1.8
0 mM
0.05 mM
0.1 mM
0.2 mM
0.4 mM
0.5 mM
1.0 mM
1.5 mM
Absorbance (au)
0.0
0.1
0.2
0.3
0
2
4
6
8
10
Time (μs)

150

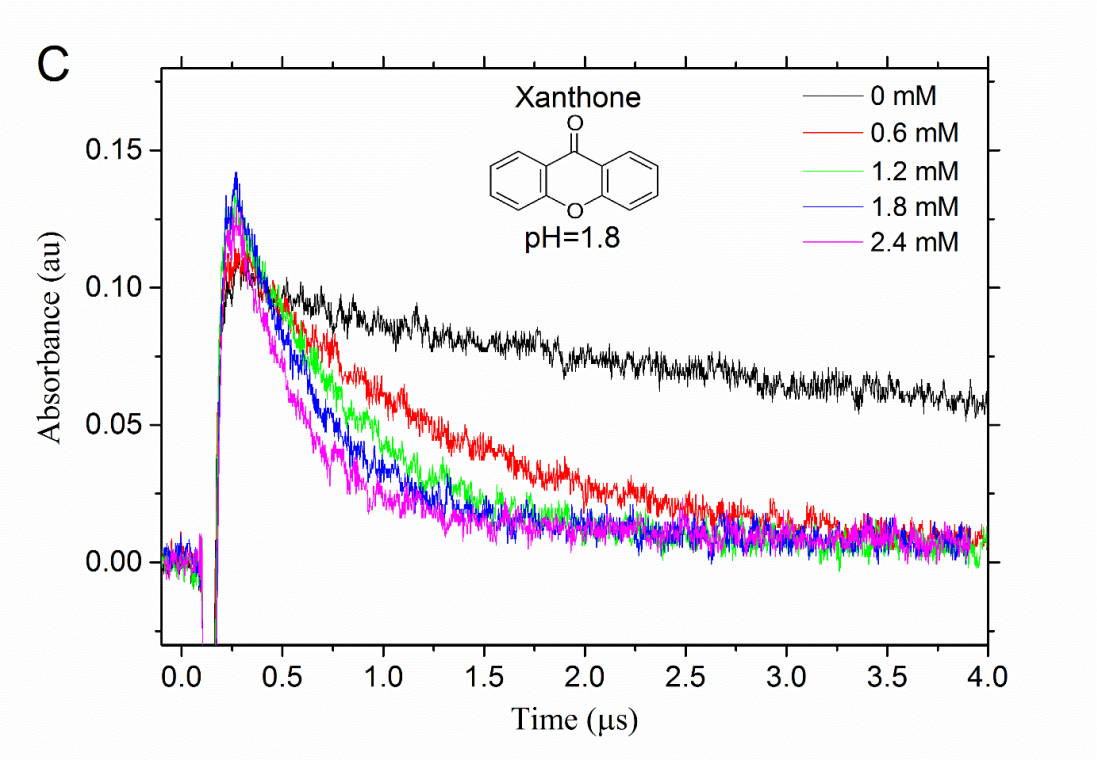
C
Xanthone
pH=1.8
0 mM
0.6 mM
1.2 mM
1.8 mM
2.4 mM
Absorbance (au)
Time (μs)

151

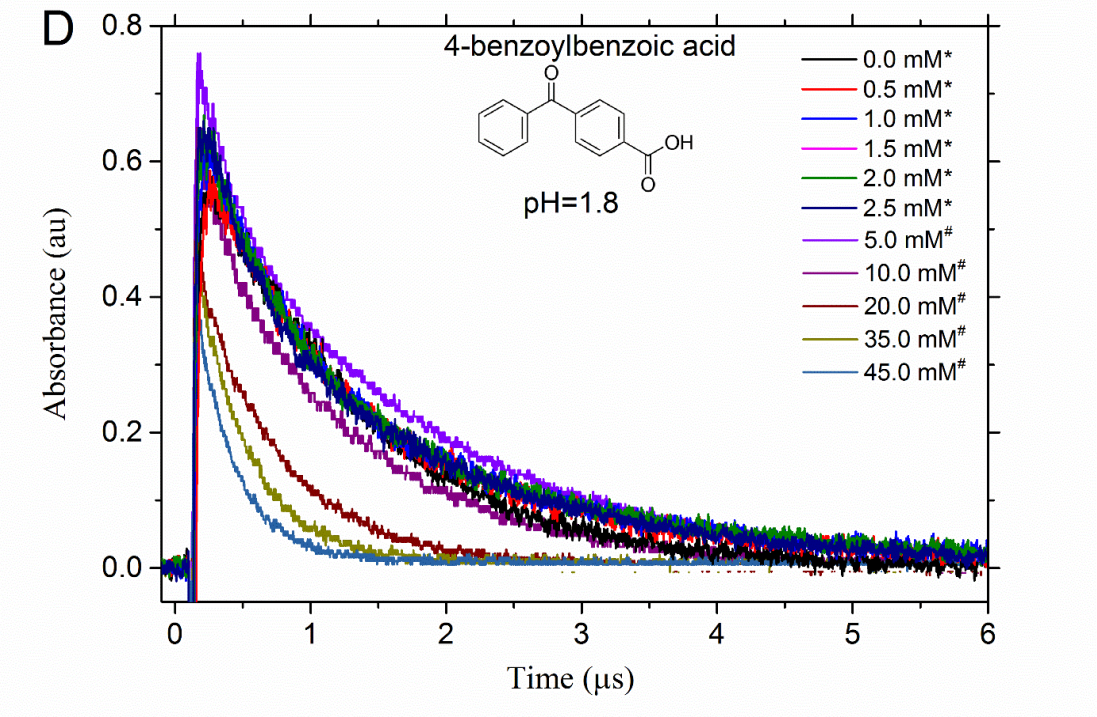
D
4-benzoylbenzoic acid
pH=1.8
0.0 mM*
0.5 mM*
1.0 mM*
1.5 mM*
2.0 mM*
2.5 mM*
5.0 mM#
10.0 mM#
20.0 mM#
35.0 mM#
45.0 mM#
Absorbance (au)
Time (μs)

152

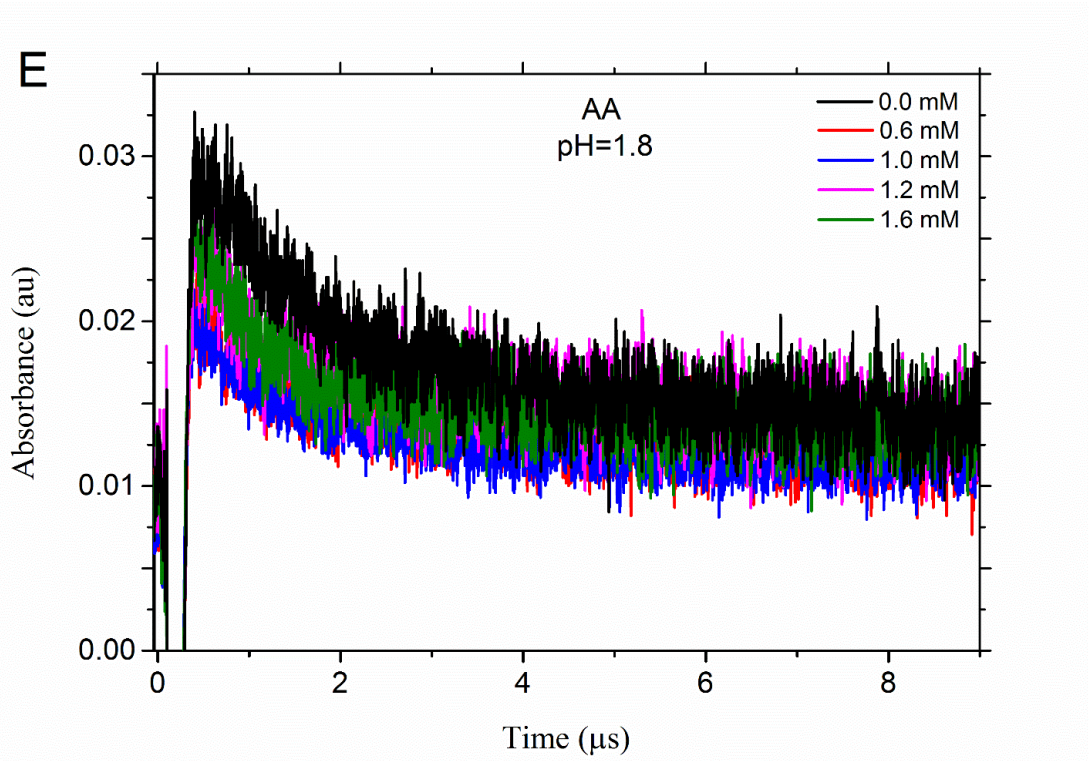

Fig. S4. Transient absorption decay of the (A) acetophenone, (B) flavone, (C) xanthone, (D) 4-BBA, and (E) AA (Extracts from the ambient samples) triplet state in deoxygenated aqueous solutions with different concentrations of Na_2SO_3 at same pH, respectively. The 4-BBA concentrations were 40 μM (*) and 20 μM ($^{\#}$), respectively, and the experiments with low concentrations of sulfite were used to make the Stern-Volmer plot and calculate the rate coefficient for the 4-BBA triplet state with hydrated SO_2.

Table S1: The rate coefficients for the quenching processing by the hydrated SO_2 and bisulfite based on regression analysis.

Photosensitizer	$k_{q(SO2\cdot H2O)}$ (M^{-1} s^{-1})	$k_{q(HSO3-)}$ (M^{-1} s^{-1})	k_0 (M^{-1} s^{-1})	Standard deviation	Multiple R	Significant F
Flavone	7.0E+08	1.5E+08	2.7E+05	6.2E+04	9.8E-01	3.2E-05
Xanthone	4.9E+08	2.1E+09	2.5E+05	9.3E+04	9.9E-01	6.1E-11

Table S2: Parameter settings used for processing the LC-MS raw data from negative mode measurements using the MZmine 2.33 software package.

1) mass detection		
	Raw data files	All
	Retention time	0 – end (auto range)
	MS level	1
	Spectrum type	Any
	Mass detector	*Wavelet transform:*
		Noise level = 500
		Scale level = 5
		Wavelet window size = 30%
	Mass list name	Masses
2) FTMS shoulder peaks filter		
	Raw data files	All
	Mass list	Masses
	Mass resolution	140 000
	Peak model function	Lorentzian
	Suffix	Filtered
	Remove original peak list	Off
3) ADAP chromatogram builder		
	Raw data files	All
	Retention time	1.5 – end
	Mass list	Masses filtered
	Min group size in b of scans	6
	Group intensity threshold	100
	Min highest intensity	1000
	m/z tolerance	0.001 *m/z* (and 0 ppm)
	Suffix	chromatograms
4) order peak lists alphabetically		
5) Chromatogram deconvolution		
	Peak lists	All
	Suffix	Deconvoluted
	Algorithm	*Wavelets (ADAP)*
		S/N threshold = 10
		S/N estimator = Intensity window SN
		Min feature height = 1000
		coefficient/area threshold = 120
		Peak duration range = 0.05 – 1.00
		RT wavelet range = 0.00 – 0.10
	m/z range for MS2 scan pairing	Off
	RT range for MS2 scan pairing	Off
	Remove original peak list	Off
6) CAMERA search		
	Peak lists	Those created by previous batch step
	FWHM	0.2
	FWHM percentage	60%
	Isotopes max charge	2
	Isotopes max per cluster	4
	Isotopes mass tolerance	0.003 *m/z* (and 0 ppm)
	Correlation threshold	0.75
	Correlation p-value	0.05
	Ionization polarity	Negative
	Do not split isotopes	Off

	Order	Perform shape correlation before isotope search
	Create new list	On
	Group peaks by	Isotope ID
	Include singletons	On
	Suffix	CAMERA
	R engine	R caller
7) Order peak lists alphabetically		
8) Join aligner		
	Peak lists	Those created by previous batch step
	Peak list name	Aligned peak list
	m/z tolerance	0.001 *m/z* (and 0 ppm)
	Weight for *m/z*	3
	Retention time tolerance	0.5 min (absolute)
	Weight for RT	2
	Require same charge state	Off
	Require same ID	Off
	Compare isotope patter	On
		Tolerance = 0.005 *m/z* (and 0 ppm)
		Min absolute intensity = 100
		Minimum score = 0%
9) clear peaklist annotations		
10) formula identification		
	Charge	1
	Ionization type	[M–H]–
	Peak lists	Aligned peak list
	m/z tolerance	0.0 *m/z* or 2 ppm
	Elements	
		C = 1 – 40
		H = 0 – 100
		O = 0 – 40
		N = 0 – 5
		S = 0 – 3
	Element count heuristics	On
		H/C ratio = On
		NOPS/C ratio = On
		Multiple element counts = On
	RDBE restrictions	On
		Range = 0 – 25
		Must be an integer = On
	Isotope pattern filter	On
		Tolerance = 0.005 *m/z* (and 0 ppm)
		Min absolute intensity = 100
		Minimum score = 0%
	MS/MS filter	Off
11) export to csv file		

Table S3: Parameter settings used for processing the LC-MS raw data from positive mode measurements using the MZmine 2.33 software package.

1) mass detection		
	Raw data files	All
	Retention time	0 – end (auto range)
	MS level	1
	Spectrum type	Any
	Mass detector	*Wavelet transform:*
		Noise level = 500
		Scale level = 5
		Wavelet window size = 30%
	Mass list name	Masses
2) FTMS shoulder peaks filter		
	Raw data files	All
	Mass list	Masses
	Mass resolution	140 000
	Peak model function	Lorentzian
	Suffix	Filtered
	Remove original peak list	Off
3) ADAP chromatogram builder		
	Raw data files	All
	Retention time	1.5 – end
	Mass list	Masses filtered
	Min group size in b of scans	6
	Group intensity threshold	100
	Min highest intensity	1000
	m/z tolerance	0.001 *m/z* (and 0 ppm)
	Suffix	chromatograms
4) order peak lists alphabetically		
5) Chromatogram deconvolution		
	Peak lists	All
	Suffix	Deconvoluted
	Algorithm	*Wavelets (ADAP)*
		S/N threshold = 10
		S/N estimator = Intensity window SN
		Min feature height = 1000
		coefficient/area threshold = 120
		Peak duration range = 0.05 – 1.00
		RT wavelet range = 0.00 – 0.10
	m/z range for MS2 scan pairing	Off
	RT range for MS2 scan pairing	Off
	Remove original peak list	Off
6) CAMERA search		
	Peak lists	Those created by previous batch step
	FWHM	0.2
	FWHM percentage	60%
	Isotopes max charge	2
	Isotopes max per cluster	4
	Isotopes mass tolerance	0.003 *m/z* (and 0 ppm)
	Correlation threshold	0.75
	Correlation p-value	0.05
	Ionization polarity	Positive
	Do not split isotopes	Off

	Order	Perform shape correlation before isotope search
	Create new list	On
	Group peaks by	Isotope ID
	Include singletons	On
	Suffix	CAMERA
	R engine	R caller
7) Order peak lists alphabetically		
8) Join aligner		
	Peak lists	Those created by previous batch step
	Peak list name	Aligned peak list
	m/z tolerance	0.001 *m/z* (and 0 ppm)
	Weight for *m/z*	3
	Retention time tolerance	0.5 min (absolute)
	Weight for RT	2
	Require same charge state	Off
	Require same ID	Off
	Compare isotope patter	On
		Tolerance = 0.005 *m/z* (and 0 ppm)
		Min absolute intensity = 100
		Minimum score = 0%
9) clear peaklist annotations		
10) formula identification		
	Charge	1
	Ionization type	[M+H]+
	Peak lists	Aligned peak list
	m/z tolerance	0.001 *m/z* (and 0 ppm)
	Elements	
		C = 1 – 40
		H = 0 – 100
		O = 0 – 40
		N = 0 – 5
		S = 0 – 5
	Elements (PFBHA derivative)	
		C = 1 – 40
		H = 0 – 100
		O = 0 – 40
		N = 0 – 5
		S = 0 – 5
		F = 0 – 25
	Element count heuristics	On
		H/C ratio = On
		NOPS/C ratio = On
		Multiple element counts = On
	RDBE restrictions	On
		Range = 0 – 25
		Must be an integer = On
	Isotope pattern filter	On
		Tolerance = 0.005 *m/z* (and 0 ppm)
		Min absolute intensity = 100
		Minimum score = 0%
	MS/MS filter	Off
11) export to csv file		

178

Database S1. The formula lists of organic compounds in ambient aerosol samples.

References:

1. Wang, X.; Hayeck, N.; Brüggemann, M.; Yao, L.; Chen, H.; Zhang, C.; Emmelin, C.; Chen, J.; George, C.; Wang, L., Chemical Characteristics of Organic Aerosols in Shanghai: A Study by Ultrahigh-Performance Liquid Chromatography Coupled With Orbitrap Mass Spectrometry. *J Geophys. Res. - Atm.* **2017,** *122*, (21), 11,703-11,722.
2. Cheng, Y.; Zheng, G.; Wei, C.; Mu, Q.; Zheng, B.; Wang, Z.; Gao, M.; Zhang, Q.; He, K.; Carmichael, G.; Pöschl, U.; Su, H., Reactive nitrogen chemistry in aerosol water as a source of sulfate during haze events in China. *Science Advances* **2016,** *2*, (12), e1601530.
3. Ye, C.; Liu, P.; Ma, Z.; Xue, C.; Zhang, C.; Zhang, Y.; Liu, J.; Liu, C.; Sun, X.; Mu, Y., High H_2O_2 Concentrations Observed during Haze Periods during the Winter in Beijing: Importance of H_2O_2 Oxidation in Sulfate Formation. *Environ. Sci. Technol.* **2018,** *5*, (12), 757-763.
4. Graedel, T. E.; Weschler, C. J., Chemistry within aqueous atmospheric aerosols and raindrops. *Rev. Geophys.* **1981,** *19*, (4), 505-539.
5. Ibusuki, T.; Takeuchi, K., Sulfur dioxide oxidation by oxygen catalyzed by mixtures of manganese(II) and iron(III) in aqueous solutions at environmental reaction conditions. *Atmospheric Environment (1967)* **1987,** *21*, (7), 1555-1560.